Science of the Total Environment 693 (2019) 133581

Contents lists available at ScienceDirect

Science of the Total Environment

journal homepage: www.elsevier.com/locate/scitotenv

Anthropogenic Marine Debris assessment with Unmanned Aerial Vehicle imagery and deep learning: A case study along the beaches of the Republic of Maldives

L. Fallati [a,b,1], A. Polidori [c,1], C. Salvatore [c], L. Saponari [a,b], A. Savini [a,b,*], P. Galli [a,b]

[a] Department of Earth and Environmental Sciences, University of Milan-Bicocca, Milan, Italy
[b] MaRHE Center (Marine Research and High Education Center), Magoodhoo Island Faafu Atoll, Maldives
[c] DeepTrace Technologies S.R.L., Milan, Italy

HIGHLIGHTS

- Unmanned Aerial Vehicle (UAV) offers a fast and reliable survey methodology.
- UAV used for Anthropogenic Marine Debris (AMD) monitoring
- Spatial resolution achieved allowed to detect high percentage of AMD on the shores.
- Deep-learning based software automatically detects and quantifies AMD.

GRAPHICAL ABSTRACT

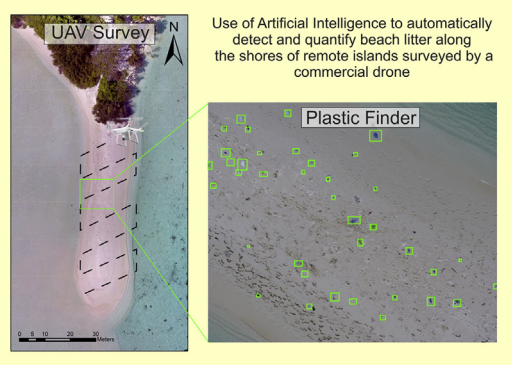

ARTICLE INFO

Article history:
Received 31 May 2019
Received in revised form 17 July 2019
Accepted 23 July 2019
Available online 24 July 2019

Editor: Damia Barcelo

Keywords:
Anthropogenic Marine-Debris
Unmanned Aerial Vehicles
Machine learning
Deep learning algorithms
Maldives
Beach

ABSTRACT

Anthropogenic Marine Debris (AMD) is one of the major environmental issues of our planet to date, and plastic accounts for 80% of total AMD. Beaches represent one of the main marine compartment where AMD accumulates, but few and scattered regional assessments are available from literature reporting quantitative estimation of AMD distributed on the shorelines. However, accessing information on the AMD accumulation rate on beaches, and the associated spatiotemporal oscillations, would be crucial to refining global estimation on the dispersal mechanisms.

In our work, we address this issue by proposing an ad-hoc methodology for monitoring and automatically quantifying AMD, based on the combined use of a commercial Unmanned Aerial Vehicle (UAV) (equipped with an RGB high-resolution camera) and a deep-learning based software (i.e.: PlasticFinder). Remote areas were monitored by UAV and were inspected by operators on the ground to check and to categorise all AMD dispersed on the beach. The high-resolution images obtained from UAV allowed to visually detect a percentage of the objects on the shores higher than 87.8%, thus providing suitable images to populate training and testing datasets, as well as gold standards to evaluate the software performance. PlasticFinder reached a Sensitivity of 67%, with a Positive Predictive Value of 94%, in the automatic detection of AMD, but a limitation was found, due to reduced sunlight

* Corresponding author.
E-mail address: alessandra.savini@unimib.it (A. Savini).
[1] These two authors equally contributed to the work.

https://doi.org/10.1016/j.scitotenv.2019.133581

conditions, thus restricting to the use of the software in its present version. We, therefore, confirmed the efficiency of commercial UAVs as tools for AMD monitoring and demonstrated - for the first time - the potential of deep learning for the automatic detection and quantification of AMD.

1. Introduction

Environmental contamination generated by Anthropogenic Marine-Debris (AMD) represents one of the most ubiquitous and long-lasting environmental change of our planet (Laist, 1987; Ryan, 2015). AMD is responsible of several ecological, ecotoxicological, economic and social impacts. However, the extent to which it is harming wildlife and plants, endangering human health and reducing the availability of ecosystem good and services (Laist, 1987; Rochman et al., 2013; Hengstmann et al., 2017) is still to be properly understood and quantified (Eriksen et al., 2014; Thompson et al., 2009). It has been estimated that from 5 to 13 million tonnes of litter enter the oceans each year (Jambeck et al., 2015; Geyer et al., 2017) and that plastic accounts for over 80% of the total AMD (UNEP, 2005; Laist, 2011; Thiel et al., 2013; Penca, 2018).

Plastic is persistent and for the most part (roughly 60%) less dense than seawater (Andrady, 2011; Ryan et al., 2009). Once introduced into the marine environment from multiple sources (both sea- and land-based), buoyant plastic can be transported by surface currents and winds (Kako et al., 2010), recaptured by shorelines (Kako et al., 2014) or degraded into microplastic (Barnes et al., 2009; Cinner et al., 2018). Distribution and accumulation of plastic into the marine environment are indeed controlled by circulation patterns and prevailing winds, coastal and seafloor geomorphology (Barnes et al., 2009; Galgani et al., 2000; Savini et al., 2014) and anthropogenic activities (Ramirez-Llodra et al., 2013). Well known hotspots of accumulation include the sea surface, where aggregations of a large amount of persistent and light plastic take place at ocean gyres, creating giant "garbage-patches" (Eriksen et al., 2014; Law et al., 2010, 2014), but also submarine canyons, where litter originating from land accumulates in large quantities (Pierdomenico et al., 2019) and the shores, particularly beaches (Corcoran et al., 2009). Although data documenting the occurrence of plastic everywhere in the oceans (from the surface to the deep seafloor - Thompson et al., 2004 and Van Cauwenberghe et al., 2013) are quite exhaustive, a consistent quantification of the total amount accumulated within the diverse marine compartments, has not been accurately outlined. While reliable estimations have been provided for the giant surface garbage-patches (Lebreton et al., 2018; Eriksen et al., 2014), scarce information is available from the deep and poorly unexplored seafloor, but nonetheless for the shorelines, where only a few and scattered regional assessments were provided (Martin et al., 2018; Vlachogianni et al., 2018; Andrades et al., 2016; Ebbesmeyer et al., 2012). Plastic accumulation on beaches may represent the terminal phase of oceanic transport or a transient stage with a successive washed to the sea following storms or tides movements (e.g. Shimizu et al., 2008). Knowing the accumulation rate on beaches and associated spatiotemporal oscillations would be a crucial information to refine global estimation on the dispersal mechanisms of plastic in the marine environment and its amount in each compartment. Most of our knowledge on the quantity of plastic accumulated on beaches, at different temporal scales, is based on sparse and regional monitoring activities, performed following different protocols and without standardized procedures, making difficult data integration and comparisons among regions (e.g. Galgani et al., 2015; Watts et al., 2017). Beach litter estimation, at places performed within the framework of dedicated monitoring activities (among others the Marine Strategy Framework Directive - Directive 2008/56/EC – Galgani et al., 2014), is also commonly subjective and time-labour consuming, since it relies on visual census where items are recorded along transects (Lavers et al., 2016; Lavers and Bond, 2017). Only recently the use of aerial imagery has been proved to be an appropriate and efficient method to monitor beach litter (Kako et al., 2012; Kataoka et al., 2018; Sha et al., 2018; Deidun et al., 2018). In particular, the use of Unmanned Aerial Vehicles (UAVs) equipped with RGB cameras, beside the advantage of the low-cost, allows the collection of high resolution imagery data (i.e.: at centimetre level - Casella et al., 2016; Flynn and Chapra, 2014) over quite large areas (e.g. hundreds of hectares), also not easily accessible, with great flexibility in terms of time and frequency of data collection (i.e. decades of hectares per day), and under conditions where satellites would be of limited use (i.e.: high cloud cover, limited image resolution). Nevertheless, estimation of beach litter from RGB imagery of various sources (UAVs included), over large and even remote areas, still requires standardization of sampling techniques and data processing. Also, objective identification of plastic items on aerial imagery, based on automatic image classification is a novel field of investigation. To the best of our knowledge, only one work has been recently published on the use of UAV Remote Sensing combined to Artificial Intelligence (AI) for beach-litter monitoring by Martin et al. (2018). They proved the ability of machine learning (ML) in performing less time-labour consuming (40 times faster than humans) and subjective methodologies to detect AMD, but the best sensitivity reported in Martin et al. (2018) for AMD automatic quantification was low (i.e.: 44%).

In our study, we therefore focused on the improvement of the sensitivity of the AI algorithm and the associated positive predicted values, which account for the false positive AMD. For this purpose, we provided a deep learning, rather than a random-forest, machine-learning approach, as previously implemented by Martin et al. (2018), being deep learning more beneficial for object detection (LeCun et al., 2015; Chollet, 2017; Guest et al., 2018). An essential output of our work is, in addition, the formulation of a combination of protocols to automatically detect and quantify beach litter along the shores of selected remote islands in the Republic of Maldives, defined by the 2010 UNPD's Assessment of Development Results a vulnerable "Small Island Developing State (SIDS)". The protection of the environment from pollution is indeed extremely important for SIDS as, aside from other reasons that are common to all countries, two important industries (tourism and fisheries) depend on a pristine environment (UNEP, 1999).

Our study proposes an ad-hoc combination of protocols to: 1) collect UAV-images suitable for the training of a deep-learning algorithm, 2) provide smart gold standards to estimate the algorithm performances, 3) train and test the deep-learning algorithm in near real-time conditions. We believe that our work could be useful to propose new best-practices for applying deep learning to automate the procedure of litter detection and quantification by UAV systems on beaches, which in turn could offer an instrumental tool for sustainable solid waste management.

2. Materials and methods

2.1. Study area

The case-study area consists of different islands of the Republic of Maldives (Fig. 1a), an archipelago composed of 1192 atoll islands stretched for 860 km, in North-South direction, located in the middle of the Indian Ocean. The islands are grouped in 20 administrative atolls and divided under three distinct categories: inhabited, uninhabited and

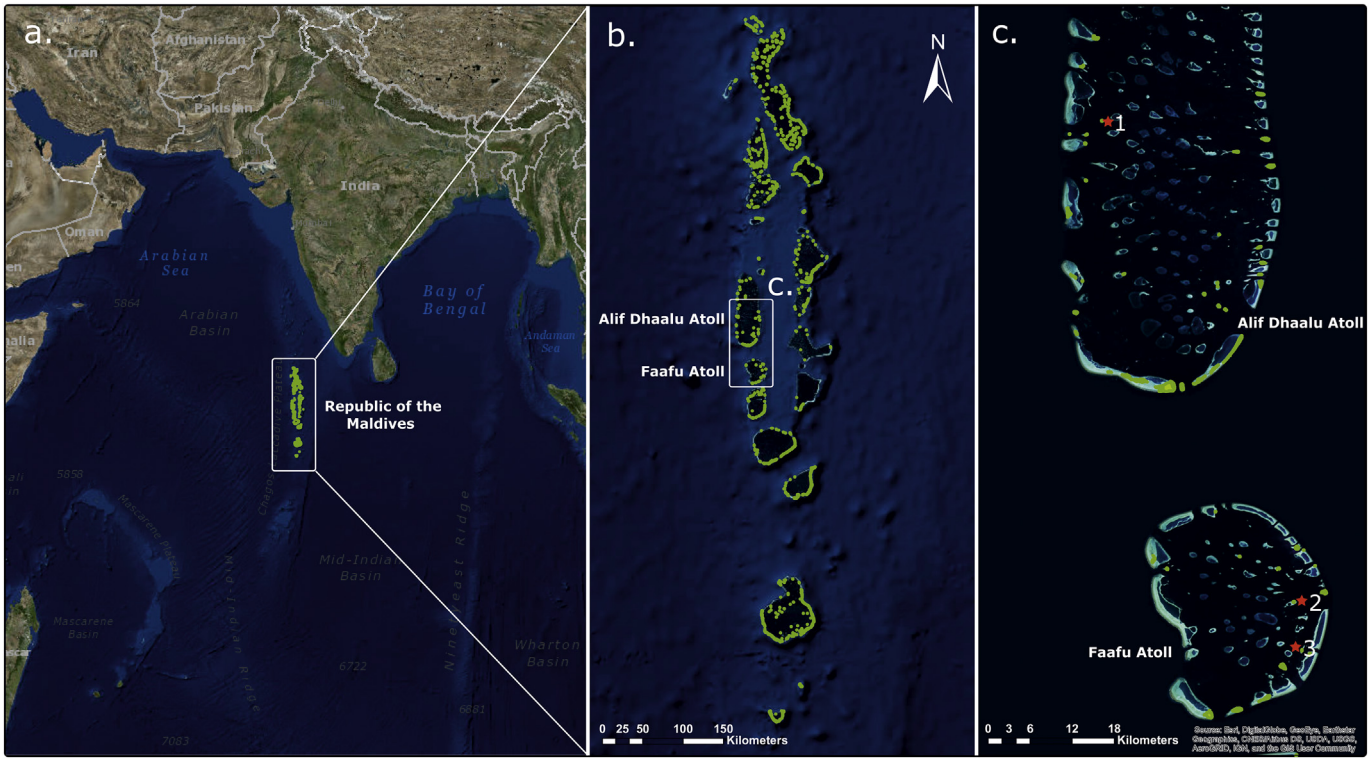

Fig. 1. Geographic location of the study area, Republic of Maldives (a.), Alif Dhaalu and Faafu Atolls (b.), and islands selected as testing sites (c.): 1 En'Boodhoo, 2 Jinnathuga, 3 Adangau.

Fig. 2. Debris accumulation in the Maldives: (a) one of the ferries port in Malè (capital city) with evident accumulation of plastic bottles released in the ocean from the boats or from the streets of the city; (b) Litter and plastic debris accumulated near the shore of Thilafushi, the only landfill island of the archipelago; (c, d) plastic waste deposited by the high tide on the beach of Adangau; (e, f) plastic waste deposited in the bushes and on the shores of En'Boodhoo.

resort islands (Fallati et al., 2017). The archipelago, with its peculiar geographical location and its 644 km of coastline, represents the perfect place for the deposition of plastic debris that are drifted from the surface currents of the Indian Ocean (Barnes, 2004). In addition, local sources of littering are represented by the waste production on the inhabited islands and those discharged into the sea from the numerous boats that daily cross the atolls. In the Maldives, the high dispersion of land mass and population, both of them spread over a distance of 860 km, creates a negative effect on solid waste management issue. With the exception of resort islands, which represent the 6% of the total archipelago surface and where beach clean-up is a daily routine operated by resort employees, most part of the coastline of each Maldivian island, is indeed covered, to an undefined extent, by AMD coming from different sources (Fig. 2).

As testing regions for our study, we selected three different coastal areas. Two of these islands (Adangau and Jinnathuga) are in Faafu Atoll, one (En'Boodhoo) is in Alif Dhaalu Atoll (Fig. 1b, c). The three islands were chosen as representatives of small-size uninhabited islands of the archipelago, where beach-cleaning cannot be guaranteed by resort employees or government personnel. En'Boodhoo is an island of 1.8 ha, located in the western lagoon of Alif Dhaalu Atoll. The island is desert, and the human presence is mainly related to the safari boats that stop nearby, and to touristic picnic and barbeques on the beach. Adangau (1.1 ha) and Jinnathuga (1.9 ha) are two islands of Faafu Atoll located in the Atoll's eastern lagoon. These two are similarly used as picnic island from the inhabitants of the Atoll. The primary sources of litter on these islands are both the direct release of waste and oceanic transport. The target testing area within the islands was selected as a portion of the beach with direct access to the sea, different exposition to the winds and currents, with the presence of psammophytes plants and natural debris (leaves, roots and twigs) as well as litter.

2.2. Aerial surveys

2.2.1. UAV

In order to achieve large-scale reproducibility of a protocol to collect UAV images, we propose to use a consumer-grade UAV, equipped with a high-resolution RGB camera, to survey the study area. For this purpose, we used the DJI Phantom 4 drone, a quadcopter with high sensing qualities, equipped with a 1/2.3″ CMOS camera sensor (12.4 MP) that can collect images with a resolution (R) of 4000 × 3000 pixels and an integrated GPS/GLONASS system. Compared to fixed-wing UAVs, that can cover with a single flight a larger area and can handle a higher quality camera, Phantom 4 is lightweight, easy to carry, and can smoothly fly at low altitude to obtain good ground-resolution images. Moreover, easy take off and landing procedures make this drone an outstanding, cost-effective solution for low altitude and short-range studies. All the metadata are recorded in an EXIF (Exchangeable Image File Format) file, which includes information on the pictures such as shutter speed, apertures, ISO and GPS coordinates (latitude, longitude and altitude). Flight time with a single battery is roughly 25 min.

2.2.2. UAV survey protocols

Three different altitudes, namely 10, 15 and 35 m were considered to define the optimal protocol in terms of image quality and number of images required to cover the area of interest (AOI):

1) ground sample distance (GSD) being defined as:

$$GSD\ mm/pix = \frac{SW \times FH}{FL \times IW}$$

where SW is the sensor width, FH is the flight high, FL is the focal length of the camera, and IW is the image width (Ventura et al., 2018), and

2) number of images of interest (IOI) being defined as:

$$IOI = \frac{AOI\ [m^2]}{D\ [m^2]} = \frac{AOI\ [m^2]}{R\ [pixels^2]\ \ GSD^2\ [m^2/pixels^2]}$$

where D is the dimension of the area covered by a single image at a specific GSD, and R is the resolution in terms of pixel of the images, as defined in Section 2.2.1.

The surveys were planned using DJI GS PRO (www.dji.com/it/ground-station-pro) a free Ipad application released by DJI. This app allows designing all the aspects of the drone mission: generate optimal flight paths, set camera parameters and directly monitor data acquisition on the Ipad screen. For all the surveys we set a fix flight altitude with a frontal and lateral overlap of 80% and 70%, respectively, a −90° gimbal angle (nadir orientation), a shooting interval of 2 s (equal time interval mode) and a constant velocity of 1.3 m/s. Before starting the UAV overflight weather condition (wind speed, cloud coverage) and the presence of obstacles along the path was checked. A metric tape was laid on the beach (e.g. for several meters), in order to check the spatial accuracy of the orthomosaic during the postprocessing. Once all the parameters were set, the UAV automatically took off and completed the mission (e.g. trajectory in Fig. 3a, b).

2.2.3. Reconstruction of the AOI

The images were processed by Agisoft PhotoScan (www.agisoft.com), a commercial Structure from Motion (SfM) software, widely used by the scientific community for its user-friendly interface, spontaneous workflow and the excellent quality of the point cloud output (Burns and Delparte, 2017; Cook, 2017; Bonali et al., 2019). The process is dived in three main steps (Fig. 3c): drone photos alignment using high accuracy setting; high-quality dense 3D point cloud generation; creation of a Digital Terrain Model (DTM) from the dense could. As final outputs we obtained, from the DTM, orthomosaics with a GSD of 4.4 mm/px, 8.2 mm/pix and 14 mm/pix respectively for the three flights altitude (10, 15 and 35 m). The models are geo-referenced thanks to the coordinates stored into the EXIF files of each image. For more extensive information on the process, see Verhoeven (2011) and Ventura et al. (2016). The orthomosaics generated from images collected at 10 m altitude, were considered as our AOI and used for data assessment.

2.3. Gold standards

2.3.1. In-situ ground assessment

We performed an in-situ ground assessment (GA) of the AOI, aimed at quantifying the AMD on the studied shorelines in order to calculate the efficiency of the UAV survey-protocols. This quantity represents our first Gold Standard (GA-GS). As a first step, a recognition of the investigated shorelines was conducted to detect AMD. The items found during the inspection were counted and classified by the operators into different subtypes (Table 1). The category named “other” refers to objects and fragments that were smaller than 5 cm, which is the minimum size of the target objects that we decided when defining the optimal protocol described in terms of the image quality. Then, these objects were re-arranged in the specific AOI to be monitored by UAV overflights.

2.3.2. Image screening

In order to evaluate the quality of the images, a comparison was made between the number and type of items counted by the operators during the in-situ GA on the beach, and the number and type of items counted by an operator during an image screening (IS) of the orthomosaic on a PC. The AMD recognised via IS represents our second GS (IS-GS), and a smart best-estimate of the actual GA-GS. Indeed, proving the feasibility of identifying and estimating the AMD by screening

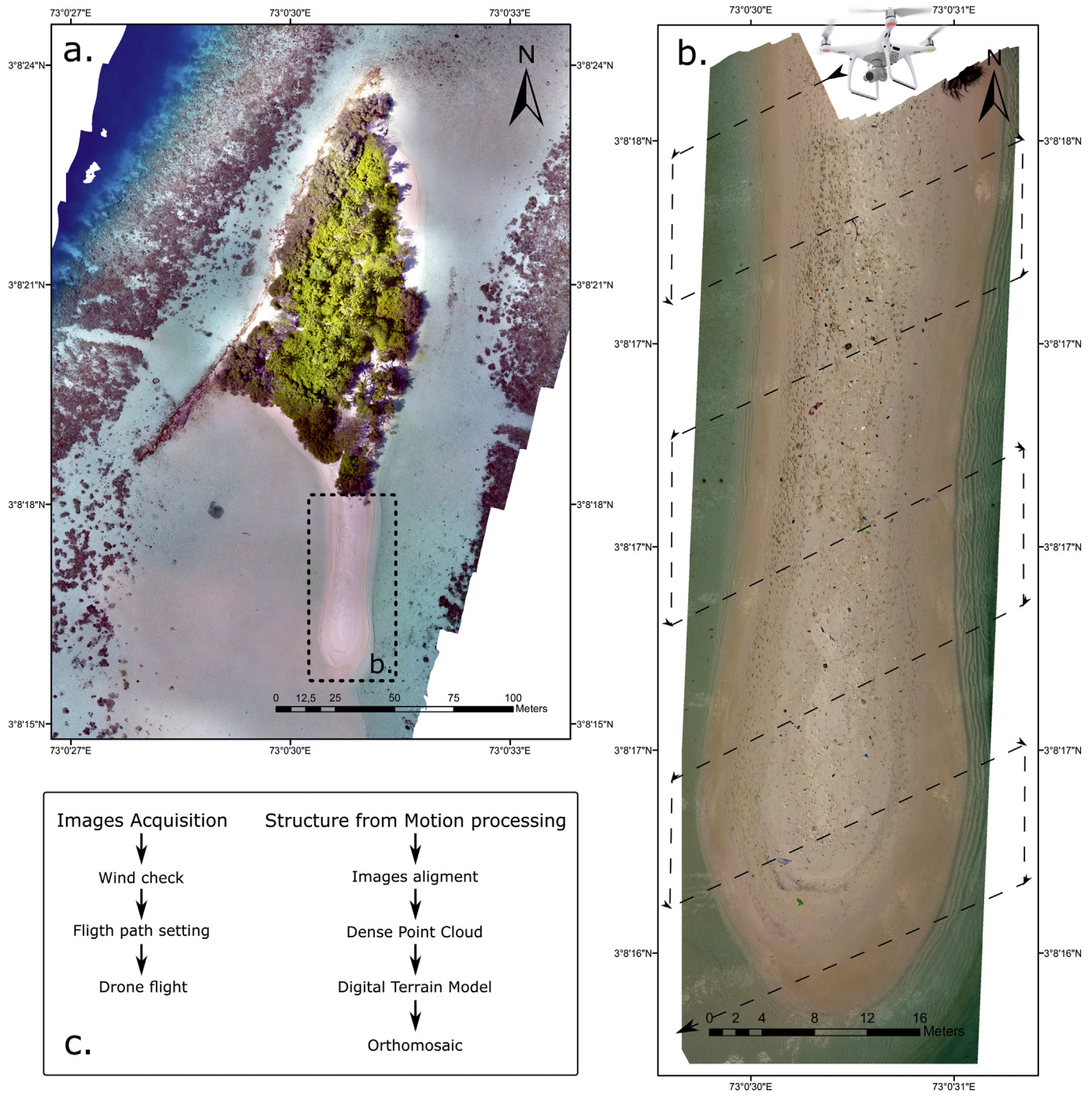

Fig. 3. Drone survey over Adangau (a.) sandy long beach. The path followed by the drone (b.) is overlayed on the high-resolution orthomosaic that was generated applying the SfM workflow (c.) to RGB images.

images collected by UAVs, rather than by operators on the ground, is crucial to choose the optimal UAV survey-protocol for the collection of images suitable for deep learning, and to establish procedures that allow avoiding the time-consuming GA of the operators.

2.4. The deep-learning algorithm

In order to allow easy access to AI non-expert users, we used a commercial software – PlasticFinder (Italian software license 012677 D011755, DeepTrace Technologies, www.deeptracetech.com/) – to detect and quantify AMD. The core algorithm of the software is a deep-learning convolutional neural network (CNN). CNNs are a class of multilayer architecture suitable for processing RGB images for classification and object detection tasks, where the stack of convolutional layers allows for translation invariance - i.e. the net is trained to recognize an object independently of its position within the image.

The adoption of a deep learning approach has one main motivation. In order to provide a tool that could favour a scalable approach, i.e. adaptable to different scenarios, a large image-database was needed to provide a general training set, i.e. a set of images to let the algorithm learn the classes of interest. The main advantage of deep learning is that it automates the most critical part of a ML workflow: the feature extraction. In contrast to conventional ML methods (e.g. Random Forest, Support Vector Machine, Gradient Boosting Machines), that require

Table 1
AOI, number of minimum IOI, climate, light and weather conditions of each investigated Maldivian island during the UAV survey and the in-situ ground assessment (GA). The number of items collected during the GA on each beach is listed per each class, and the items identified via image screening (IS) via PC are also reported.

	Jinnathuga		Adangau		En'Boodhoo	
AOI (m^2)	216		1056		225	
IOI	1		5		1	
Climate (month)	April		November		October	
Light (time)	12 pm		12 pm		5 pm	
Weather (conditions)	Sunny		Sunny		Cloudy	
Use	Training set		Testing set		Testing set	
AMD class	GA	IS	GA	IS	GA	IS
Lighter	4	1	1	1	4	4
Bottle	21	21	50	54	47	43
Straw	1	0	1	0	0	0
Net	11	8	3	3	2	3
Plastic bag	7	7	43	50	3	2
Aluminum can	8	6	11	13	21	14
Plastic containers	3	3	1	1	12	7
Plastic utensils	0	0	20	8	1	0
Flip flop	1	1	13	8	32	29
Other	26	25	4	3	13	19
Total	82	72	147	141	135	120
Matching score (%)	87.8		95.9		88.8	

hand-design features as input, a neural network is made of trainable multilayers that learn automatically the features through geometric transformations and gradual adjustments of learning weights with respect to a feedback signal, thus being more suitable than conventional ML for large dataset training (LeCun et al., 2015, Chollet, 2017). The PlasticFinder CNN has been tailored for 5 classes of images, namely: "vegetation", "sea", "sand", "AMD" and "other" (i.e. sand with small pieces of wood, stones, algae). UAV images obtained from the survey of Jinnathuga island were used for the collection of the training set (Fig. 4).

The island was chosen on the basis of the fact that all the classes of interest were present. Therefore, we selected training images, within the AOI, representing the classes of interest. For each class, a balanced number - of the order of thousands – of different samples was collected, in order to tailor the algorithm on the specific experimental settings. A subsample of UAV images ($N = 3$) collected on the other two islands, Adangau and En'Boodhoo, were used for the testing set. The surveys of the testing-set islands were finalised at different experimental conditions (Table 1) which allowed investigating the influence of climate, light and shadow on the efficacy of the algorithm. When a tested image is input in the software, it returns pixel-wise classification heatmaps, representing a pixel probability-map for each class, and a bounding-boxes map with the detected AMD.

The performance of the automatic detection, classification and quantification were measured by comparing the results with the two GS. The metric is expressed in terms of true positive (TP), false negative (FN) and the false positive (FP) items, rather than in terms of pixels, for an easier interpretation. The statistical measure of the performances is expressed through the $Sensitivity = TP / (TP + FN)$, the Positive Predictive Value $PPV = TP / (TP + FP)$, and the harmonized mean of Sensitivity and PPV, given by the $F\text{-}score = 2TP / (2TP + FP + FN)$.

3. Results

3.1. Optimization of UAV survey protocols

The optimal protocol for the UAV survey, as a compromise between image resolution and number of IOI to cover the AOI, was found at a UAV altitude of 10 m, corresponding to a GSD of 4.4 mm/pixels. The know dimension of the objects (metric tape) in the orthomosaics strongly matches the true dimensions measured on the beaches with an average accuracy of ≈1 mm. Table 1 reports the different AOI covered following the optimal protocol for three selected islands, namely Jinnathuga, Adangau and En'Boodhoo islands, and the corresponding number of minimum IOI.

3.2. Gold standards

Table 1 reports the experimental results of the in-situ GA and of the IS of the AOI. The matching scores express the ratio of the AMD found via IS to the AMD found during the GA. This score accounts for the estimated error in the use of the GS produced via IS.

3.3. The deep-learning algorithm

3.3.1. Training, testing and performance

The training of the tailored CNN, performed on images from Jinnantuga-island (Fig. 4), achieved a validation accuracy higher than 95%. Adangau and En'Boodhoo-islands images (Figs. 5a–6a) were used to test the algorithm. A pixel-wise probability heat-map of each input image has been obtained by the software, as well as a bounding-boxes map for the detected AMD (Figs. 5a–6a). In particular, for each pixel, a probability is given to be classified as AMD, thus allowing a visual understanding of the specific areas that might be subjected – with a different probability of risk exposure – to the presence of plastic debris.

Figs. 5c and 6c, shows bounding-boxes maps with all AMD detected. Table 2 reports the numerical results obtained by comparing the software output and the IS-GS for each image. The results highlight the average software-performance for En'Boodhoo drops of a factor of about 3 with respect to the Adangau case.

Therefore, these results give the evidence that the collection of UAV-images suitable for the training and testing of the deep-learning algorithm, should rely on specific recommendations regarding the optimization of the UAV survey, the collection of the GS, and the development of the algorithm itself.

4. Discussion

4.1. The UAV survey and the AMD detection

The low cost, the high resolution and the high flexibility of UAVs quickly turned out to make them extremely versatile and useful tools

Fig. 4. Examples of Jinnathuga island images (a., b. and c.), used as training set for the deep-learning algorithm. Note the presence of the different classes in the images, in particular "AMD" in (a), "sand" in (a), (b) and (c), "sea" in (b), "vegetation" and "other" in images (a) and (c).

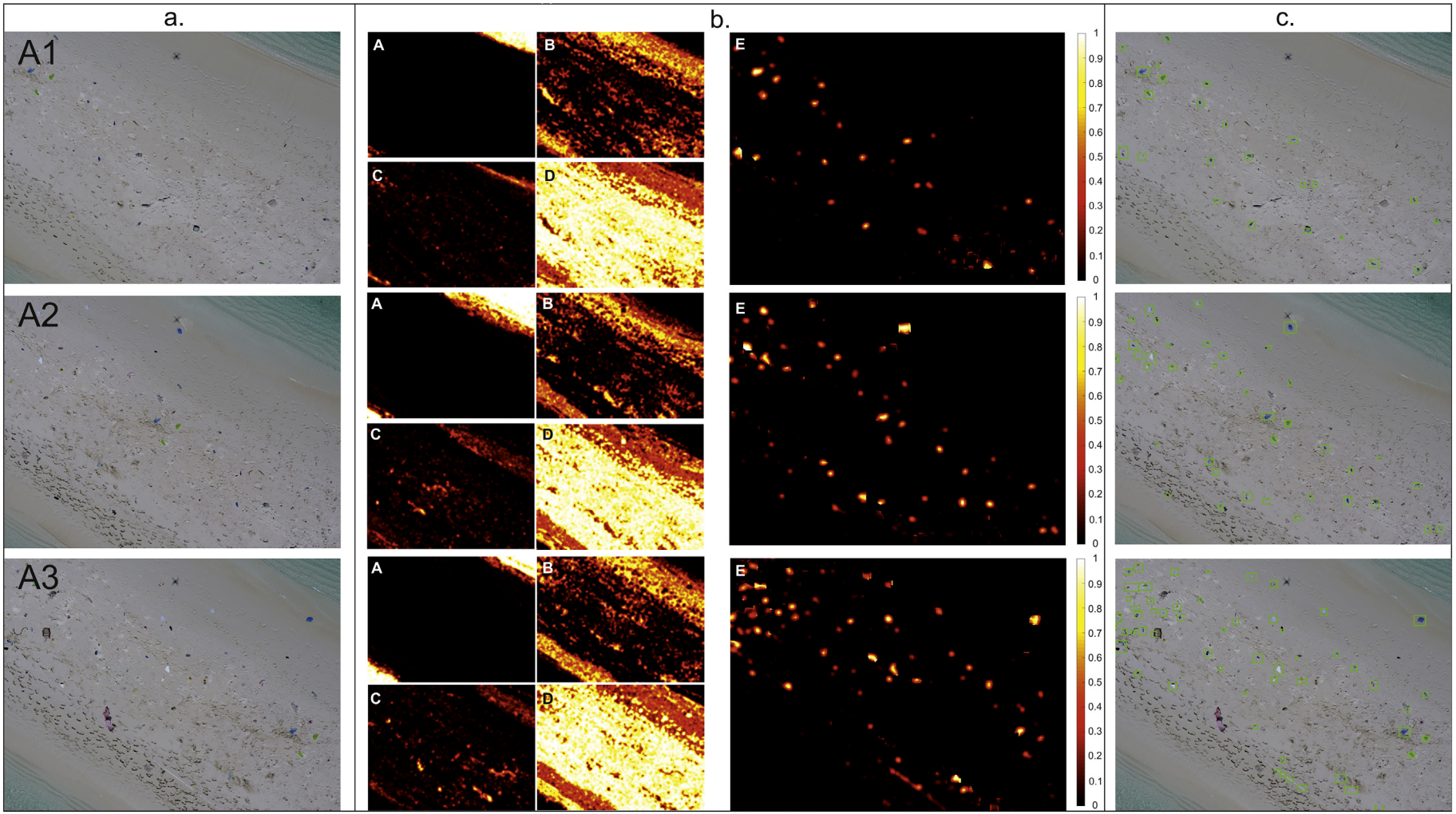

Fig. 5. Canvas on the left (a.), from top to bottom: testing-set images A1, A2 and A3 for Adangau-island. Central canvas (b.), from top to bottom: PlasticFinder pixel-wise classification heatmaps for Adangau-island images A1, A2 and A3 representing, respectively, the classes sea (A), sand (B), vegetation (C) other/AMD (D), and AMD (E) with the probability scale ranging from 0 to 1. Canvas on the right (c.), from top to bottom: PlasticFinder bounding-boxes maps for the Adangau-island images A1, A2 and A3. Each green bounding box is identified as an item of AMD by the software. (For interpretation of the references to colour in this figure legend, the reader is referred to the web version of this article.)

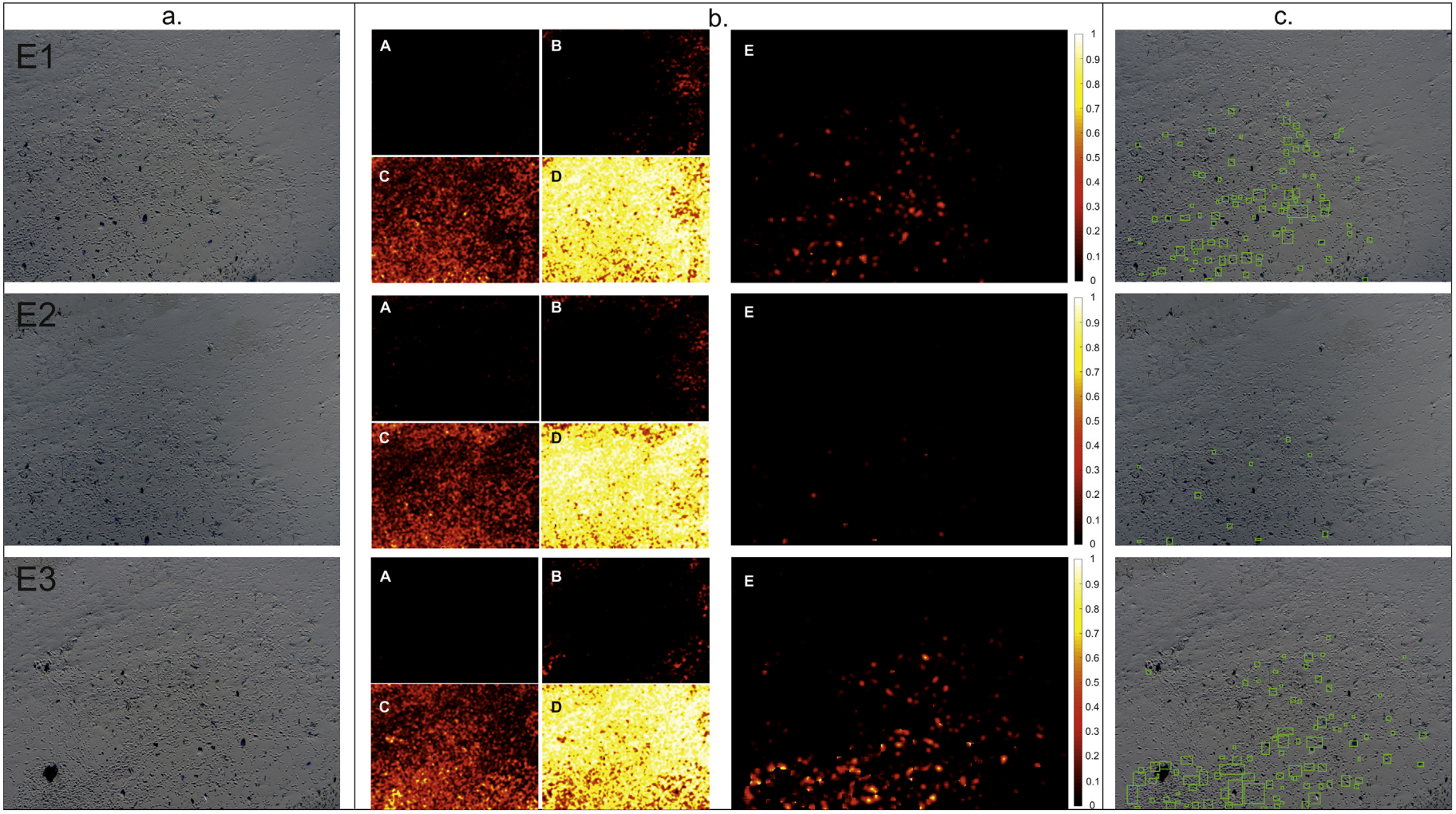

Fig. 6. Canvas on the left (a.), from top to bottom: testing-set images E1, E2, E3 for En'Boodhoo island. Central canvas (b.), from top to bottom: PlasticFinder pixel-wise classification heatmaps for En'Boodhoo-island images E1, E2, E3 representing, respectively, the classes sea (A), sand (B), vegetation (C), other/AMD (D), and AMD (E) with the probability scale ranging from 0 to 1. Canvas on the right (c.), from top to bottom: PlasticFinder bounding-boxes maps for the En'Boodhoo-island images E1, E2, E3. Each green bounding box is identified as an item of AMD by the software. (For interpretation of the references to colour in this figure legend, the reader is referred to the web version of this article.)

Table 2
Results for the Adangau and En'Boodhoo testing-set images A1, A2, A3 and E1, E2, E3, respectively. Average scores (AVG) are also given for each set. AMD accounts for the total real items in each image, as identified by the gold standard. True positive (TP), false negative (FN) and false positive (FP) items are combined to express the software performance in terms of sensitivity, PPV and F-score.

IMG	AMD	TP	FN	FP	Sensitivity (%)	PPV (%)	F-score (%)
Adangau							
A1	37	25	12	0	0.68	1.00	0.81
A2	58	40	18	4	0.69	0.91	0.78
A3	89	56	33	6	0.66	0.90	0.74
AVG	61.3	40.3	21	3.3	0.67	0.94	0.78
En'Boodhoo							
E1	71	23	48	66	0.32	0.26	0.29
E2	43	5	38	6	0.12	0.45	0.19
E3	98	25	73	65	0.26	0.28	0.27
AVG	70.6	17.6	53	45.6	0.23	0.25	0.33

for the investigation and analysis of a number of environmental issues. Small UAVs are used indeed with increasing frequency, in many research activities with applications in different fields: structural geology (Bonali et al., 2019), forestry sciences (Baron et al., 2018; Mlambo et al., 2017), mapping of sensitive marine habitats (Ventura et al., 2018), marine megafauna surveys (Colefax et al., 2018; Kiszka et al., 2016), coral bleaching detection (Levy et al., 2018). These platforms, especially the commercial drones, are proving to be useful tools for high-resolution remote sensing data collection, especially because of their small size, the increased lifetime of the batteries and the possibility to plan autonomous flights with user-friendly ground station software. Moreover, SfM algorithms allow obtaining accurate Digital Terrain Models (DTMs) and orthomosaics over large areas.

AMD was monitored worldwide through aerial surveys, along the beaches, since 2012 (Kako et al., 2012; Deidun et al., 2018; Kataoka et al., 2018; Martin et al., 2018; Sha et al., 2018) but explored locations are still limited (Fig. 7). Besides, more significant, it is the absence of a standardized protocol for data acquisition and elaboration. Previous studies, performed using a balloon equipped with a digital camera (Kako et al., 2012) and aerial photographs (Kataoka et al., 2018), faced problems related to the orthorectification and to the pixel-size of the images: a GSD of 10 cm/pix allowed identifying only groups of debris and not the single objects. The recent adoption of UAVs for AMD monitoring overcome a number of limitations mainly related to the flight altitude and to the GSD, to the orthorectification of the images, and to the repeatability of the surveys in a short time. However, the data-processing procedures are not uniform, ranging from visual interpretation of the images (Deidun et al., 2018) and spectral profile analysis of litter (Sha et al., 2018), to the use of machine learning methods (Martin et al., 2018). The use of AI classifiers (Martin et al., 2018) is more complex for different reasons, among which the lack of publicly available large databases (providing adequate images to train algorithms) is notable. The difficulty of developing scalable approaches, i.e. procedures that do not depend on local environmental constrains, is also a major issue for the use of AI classifiers.

The advantages in using UAVs, in terms both of resolution and monitoring repeatability, match perfectly with the need of understanding the pattern of aggregation in a remote area such as the Republic of Maldives. Here, a considerable amount of marine litter has been reported, despite the remoteness of the location (Imhof et al., 2017). However, Imhof et al. (2017) highlighted the need for a robust protocol, allowing extensive sampling in space and time to collect scientifically sound data (Imhof et al., 2017). Remote-sensing studies, related to the accumulation and transportation of AMD, were not conducted before this work in the Republic of Maldives (Fig. 7). The lack of such monitoring studies for this area is significant, considering that plastic debris from the rivers of South Asia contributes to 67% of the global annual input (Lebreton et al., 2017) and that countries on the Indian Ocean are among the principal producer of mismanaged plastic waste (Jambeck et al., 2015). Besides, it is not clear where all this plastic, that should accumulate in the Indian Pacific, gyre is going (Mheen et al., 2019). Thus, the proposed methodology will improve and standardise the data collection of marine-litter accumulation on beaches and shorelines, gathering valuable and comparable data, even in remote and isolated areas.

The results of our study confirm most of the advantages of using a consumer-grade drone to carry out environmental monitoring. In particular, the use of a DJI Phantom 4 drone allowed speeding up considerably the standard walking beach survey and to access remote areas such as Maldives.

On the surveyed islands, anthropogenic debris were found everywhere: on the water's edge, just left there from waves and tides; on the upper part of the beaches and in the bushy coastal vegetation, likely carried there from storm tides and winds, or left by local tourists. The selected GSD allowed the identification and categorization of debris for each single detected item, making our remote observations comparable to the ones performed by operators on the ground. In fact, the matching between the ground-assessment and the visual screening of the images is higher than 87% (Table 1). In addition, the results of our survey protocol shows that the majority of the detected objects (Table 1) were plastics bottles and aluminum cans. Particularly abundant were also flip flops on En'Boodhoo and Adangau. These three categories of debris

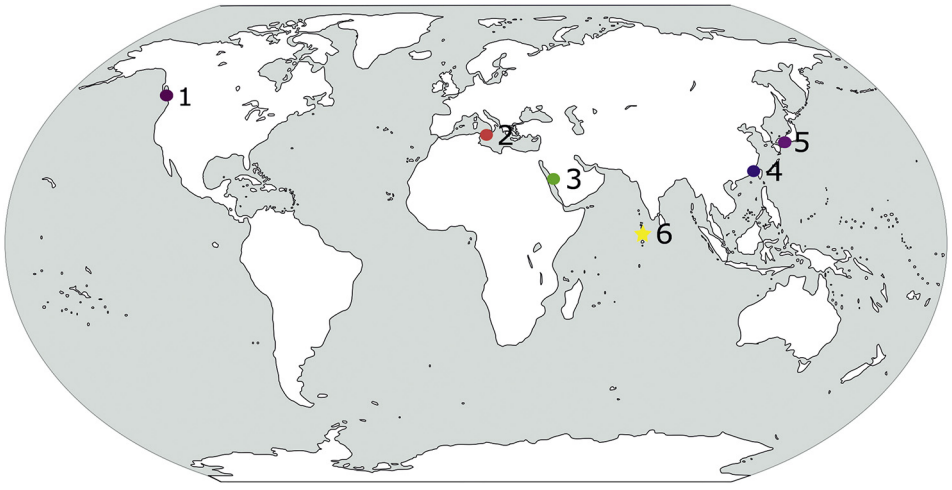

Fig. 7. Geographic distribution of studies that used remote sensing techniques to monitor and detect beach debris: 1 Vancouver Island, Canada (Kataoka et al., 2018); 2 Malta (Deidun et al., 2018); 3 Saudi Arabia (Martin et al., 2018); 4 Fuzhou, Fujian, China (Sha et al., 2018); 5 Seto Inland Sea, Japan (Kako et al., 2012); 6 Republic of Maldives, present study area.

were observed with different degradation level: from brand new, with labels and the colours still intact, to partially disrupted. This can indicate the heterogeneity of the sources: some of them can be just washed up on the shore from the closest inhabited island or discharged from boats that passed nearby; others may have float in the ocean for thousands of kilometres before reaching the shore. Instead, the higher presence of plastic bags (foods wraps and plastic bags) on Adangau island is most probably due to the use of the island as a picnic and barbeque location from the inhabitants of the atoll.

The graphical outputs and the numerical results for Adangau Island show good performances (Fig. 5, Table 2) and, in particular, in the face of an average sensitivity of 67%, the average PPV reaches 94%. This means that the deep-learning algorithm performance is affected by a non-negligible number of FN items – impacting on the sensitivity – but also that, on the other hand, the software is highly specific in the ability to recognize AMD with respect to FP items. In addition, it should be noted that, for Adangau island, the software performance is quite stable, even when the number of real AMD-items on the beach increases (Table 2). The pixel-wise classification heatmaps for En'Boodhoo-island, shown in Fig. 6b, qualitatively confirm the good ability of deep learning algorithm, in recognizing the presence or absence of elements belonging to the "sea" class. Also, the software correctly reports on a low-probability with respect to the presence of vegetation (below 30%). On the contrary, the heatmaps for the other classes draw attention to issues that become evident when looking at the zoomed bounding-boxes maps in Fig. 8, and to the quantitative results shown in Table 2. In this case, the average software-performance for En'Boodhoo drops of a factor of about 3 with respect to the Adangau case. This limitation can be explained by considering the different lighting conditions. In particular, Adangau-island images were collected at 12 am of a sunny day, therefore with similar sunlight-conditions of the testing set of Jinnathuga island. On the contrary, En'Boodhoo images were collected at 5 pm, and the shadows in the proximity of footprints (Fig.8) or of real AMD, represent pitfalls for the algorithm, as clarified by the high number of FP items in Table 2. As a matter of facts, the software was not trained to recognize footprints or shadows, and therefore such a limitation restricts the use of PlasticFinder, in its present version, to specific sunlight-conditions. For these reasons, we suggest conducting the survey with the sun high on the horizon, in order to avoid excessive shadows on the surveyed areas. However, to date, and to the best of our knowledge, there is only another algorithm presented to the scientific community, that has been developed for the specific purpose of automatically detect and quantify AMD along the shores by using a combination of UAV images and AI. In their pioneering work, Martin et al. (2018), focused their efforts in the Saudi-Arabian shorelines. They faced the highly-challenging task of both detecting and classifying the AMD typology with a series of multi-class random-forest classifiers, based on the extraction of HoG features. The authors validated the feasibility of using AI for AMD detection, but pointed out that the use of deep learning would have been more beneficial with respect to their approach that achieved a maximum sensitivity of only 44%. Therefore, our work represents the first implementation to automatically detect and accurately quantify AMD, based on a deep-learning approach. Results in Table 3 point out that PlasticFinder performances give better results, with respect to all the metrics, especially if used in the appropriate sunlight conditions. In particular, PlasticFinder PPV is much higher than the one obtained by Martin et al. (2018), allowing for a more specific tool to alarm on and quantify the presence of AMD. In fact, it is important to highlight that, in order to monitor the presence of AMD and to know which are the areas that require an urgent intervention (i.e. those where AMD accumulate the most), it is essential to have a tool that is able to detect only AMD, without mistaken false positives. To this extent, reaching a high PPV is more crucial than a high Sensitivity. Also, the fact that the reached Sensitivity is constant, despite the different loads of litter on the beach, is also a good result because it shows that the more is the AMD, the higher is the litter detected by PlasticFinder, i.e. this technology is able to detect accumulation zones.

Table 3
Comparison between results from Martin et al. (2018) (average on the overall results), PlasticFinder results for Adangau island and averaged results for Adangau and En'Boodhoo island.

Algorithm	TOT	TP	FN	FP	Sens (%)	PPV (%)	F-score (%)
Martin et al.	415	164	251	1941	0.40	0.08	0.13
PlasticFinder (Adangau)	61.3	40.3	21	3.3	0.67	0.94	0.78
PlasticFinder (AVG A/E)	131.9	57.9	74	48.9	0.44	0.54	0.49

These results reflect the major advantage of deep learning, with respect to conventional ML methods, which is the fact that it is not necessary to pre-transform data (e.g. an image) into selected features to feed models, but data can be input into neural-network models to let them automatically identify the best representations that allows tasks such as detection or classification (LeCun et al., 2015).

4.2. Best-practices optimization and future improvements

In order to optimize and enhance best practices for AMD remote-sensing monitoring, further improvements should be applied to the adopted protocols and methods.

In terms of the UAV survey, we reckon that once all the flight parameters have been set, the monitoring can be carried out from a small boat, in the proximity of the shores, without the need of reaching the beach, often inaccessible for the presence of coral reefs all around the islands. Therefore, this methodology can be particularly useful in geographical sites, such as the Maldives, where the presence of many small remote uninhabited islands, and the need to optimize the AMD beach-monitoring, represents a pressing matter.

In terms of the ground assessment protocol, such assessment is used to validate the reliability of the methodology, but, in implementing the protocol, it is not supposed to happen every time (otherwise the protocol would lose its time-efficiency). For this reason it has been not included in the Protocol recommendations (Table 4). In general, the beach should be left untouched before the UAV survey to avoid footprints or other environment manipulations that could affect the methodology performance, especially in remote places.

Another important remark is that, for a relevant fraction of the AMD, the deposition on the beach is only a transitory phase before being taken

Fig. 8. Examples of shadows in the proximity of footprints (left image) and of items of AMD (right image), that are mistaken as AMD by the software, representing pitfalls for the algorithm in its present version.

Table 4
Optimal protocol and key recommendations for the optimization of the UAV survey, the collection of gold standards and of UAV images suitable for the training and testing of a deep-learning algorithm.

UAV Survey	
Flight Altitude	10 m
GSD	4.36 mm/pix
Camera Gimbal Orientation	-90° (nadir orientation)
Images acquisition along fixed paths	80% frontal overlap 70% lateral overlap 2 s of shooting interval 1,3 m/s constant velocity
Gold Standard	
Ground Assessment	AMD inspection and subtype classification (to be limited to few representative areas for the validation of methodology) AMD Size >5 cm
Image Screening	AMD counting and subtype classification Matching Score >80%
Deep Learning	
Training	# of images per class ~ 10^3 Validation accuracy for tailored CNN >95%
Testing	# of images ~ # IOI Use IS-GS to test performances with metrics Use GA-GS to estimate error on the IS-quantified performance

up by the currents to resume the floating travel in the ocean. Instead, other AMD can be trapped on the upper part of the beach, where environmental factors and the erosive action of the sand can accelerate the plastic degradation processes. The microplastics particles (<5 mm) produced by the degradation of the AMD trapped on the upper part of the shore can enter in the sediments or can be released as contaminants in the water of the lagoon (Saliu et al., 2018; Saliu et al., 2019). Therefore, fast and efficient data collection and image analysis of the distribution of AMD on the shore, as well as specific AI tools for its automatic and objective assessment are necessary, but not sufficient, since microplastic is lost from this detection and quantification. However, the distribution and quantitation of AMD, as obtained from our protocol, could be used to understand which are the most impacted areas, and the AMD depositional seasonal trends connected to the Indian Ocean currents patterns (Mheen et al., 2019). The creation of an integrated model could allow stakeholders (e.g. governments, NGO) using this information in order to promote mitigation actions, such as specific citizenship awareness initiatives, beach–clean up events, but also addressing – with a data-driven approach - the interception of the floating AMD, before reaching the shorelines.

Finally, we would suggest some improvement for PlasticFinder, for example, by a more in-depth training, with the aim of avoiding sunlight-conditions dependence for its use, which represents, to date, one of its major limitations. Also, optimization should be implemented to scale up the algorithm speed and ability to process full orthomosaic images, overcoming time-scale limitations due to processing of a large amount of data. In Table 4, we summarize and suggest an optimal protocol, with key recommendations.

5. Conclusion

Our work was aimed at proposing an efficient and reliable monitoring protocol, to address a pressing worldwide environmental issue such as AMD deposition along the shores. Low altitude remote-sensing data are essential for obtaining a synoptic overview of extended areas, and UAVs are powerful tools to acquire them. Our study, confirmed the use of a commercial drone for AMD monitoring as a fast and reliable surveys methodology. The use of UAV is instrumental to survey remote areas and the spatial resolution achieved in the collected images allowed detecting a percentage of the objects on the shores higher than 87.8%. A deep-learning based software, PlasticFinder, has been used for the automatic detection and quantification of AMD, providing analysis of the UAV collected images. In the Maldivian case study, the overall performances were good, reaching a PPV of 94% with the better sunlight conditions, much greater than the only state-of-the-art AI algorithm so far published in literature. The only critical limitations, observed in our study, are determined by environmental circumstances encountered during the survey, and especially sunlight conditions and the associated terrain shading effects: restrictions are given for the images that can be analysed with the deep-learning algorithm in its present version, where the PPV is reduced to 54%.

Acknowledgments

The authors are grateful to MaRHE Center and Planhotel Hospitality Group, in particular, Diamonds Thudufushi Resort, for the logistic support provided during the field work.

References

Andrades, R., Martins, A.S., Fardim, L.M., Ferreira, J.S., Santos, R.G., 2016. Origin of marine debris is related to disposable packs of ultra-processed food. Mar. Pollut. Bull. 109 (1), 192–195. https://doi.org/10.1016/J.MARPOLBUL.2016.05.083.

Andrady, A.L., 2011. Microplastics in the marine environment. Mar. Pollut. Bull. 62 (8), 1596–1605. https://doi.org/10.1016/J.MARPOLBUL.2011.05.030.

Barnes, D.K.A., 2004. Surveys from Negombo in West Sri Lanka, Ari Atoll in the Maldives. Retrieved from. http://www.cordell.org/HD/HD_documents/HE_Library/Debris/RIA.pdf.

Barnes, D.K.A., Galgani, F., Thompson, R.C., Barlaz, M., 2009. Accumulation and fragmentation of plastic debris in global environments. Philos. Trans. R. Soc. B 364 (1526), 1985–1998. https://doi.org/10.1098/rstb.2008.0205.

Baron, J., Hill, D.J., Elmiligi, H., 2018. Combining image processing and machine learning to identify invasive plants in high-resolution images. Int. J. Remote Sens. 39, 5099–5118. https://doi.org/10.1080/01431161.2017.1420940.

Bonali, F.L., Tibaldi, A., Marchese, F., Fallati, L., Russo, E., Corselli, C., Savini, A., 2019. UAV-based surveying in volcano-tectonics: an example from the Iceland rift. J. Struct. Geol. https://doi.org/10.1016/j.jsg.2019.02.004.

Burns, J.H.R., Delparte, D., 2017. Comparison of commercial structure-from-motion photogrammety software used for underwater three-dimensional modeling of coral reef environments. International Archives of the Photogrammetry, Remote Sensing and Spatial Information Sciences - ISPRS Archives. vol. 42, pp. 127–131. https://doi.org/10.5194/isprs-archives-XLII-2-W3-127-2017.

Casella, E., Collin, A., Harris, D., Ferse, S., Bejarano, S., Parravicini, V., ... Rovere, A., 2016. Mapping coral reefs using consumer-grade drones and structure from motion photogrammetry techniques. Coral Reefs https://doi.org/10.1007/s00338-016-1522-0.

Chollet, F., 2017. Deep Learning With Python. 1st edition. Manning Publications Co., Greenwich, CT, USA.

Cinner, J.E., Maire, E., Huchery, C., MacNeil, M.A., Graham, N.A.J., Mora, C., ... Mouillot, D., 2018. Gravity of human impacts mediates coral reef conservation gains. Proc. Natl. Acad. Sci. 115 (27), E6116–E6125 Retrieved from. http://www.pnas.org/content/early/2018/06/12/1708001115.

Colefax, A.P., Butcher, P.A., Kelaher, B.P., 2018. The Potential for Unmanned Aerial Vehicles (UAVs) to Conduct Marine Fauna Surveys in Place of Manned Aircraft. ICES Journal of Marine Science. Oxford University Press https://doi.org/10.1093/icesjms/fsx100.

Cook, K.L., 2017. An evaluation of the effectiveness of low-cost UAVs and structure from motion for geomorphic change detection. Geomorphology 278, 195–208. https://doi.org/10.1016/j.geomorph.2016.11.009.

Corcoran, P.L., Biesinger, M.C., Grifi, M., 2009. Plastics and beaches: a degrading relationship. Mar. Pollut. Bull. https://doi.org/10.1016/j.marpolbul.2008.08.022.

Deidun, A., Gauci, A., Lagorio, S., Galgani, F., 2018. Optimising beached litter monitoring protocols through aerial imagery. Mar. Pollut. Bull. 131, 212–217. https://doi.org/10.1016/J.MARPOLBUL.2018.04.033.

Ebbesmeyer, C.C., Ingraham, W.J., Jones, J.A., Donohue, M.J., 2012. Marine debris from the oregon dungeness crab fishery recovered in the Northwestern Hawaiian Islands: identification and oceanic drift paths. Mar. Pollut. Bull. https://doi.org/10.1016/j.marpolbul.2011.09.037.

Eriksen, M., Lebreton, L.C.M., Carson, H.S., Thiel, M., Moore, C.J., Borerro, J.C., ... Reisser, J., 2014. Plastic pollution in the world's oceans: more than 5 trillion plastic pieces weighing over 250,000 tons afloat at sea. PLoS ONE https://doi.org/10.1371/journal.pone.0111913.

Fallati, L., Savini, A., Sterlacchini, S., Galli, P., 2017. Land use and land cover (LULC) of the republic of the Maldives: first national map and LULC change analysis using remote-sensing data. Environ. Monit. Assess. 189 (8), 417. https://doi.org/10.1007/s10661-017-6120-2.

Flynn, K.F., Chapra, S.C., 2014. Remote sensing of submerged aquatic vegetation in a shallow non-turbid river using an unmanned aerial vehicle. Remote Sens. 6 (12), 12815–12836. https://doi.org/10.3390/rs61212815.

Galgani, Francois, Ryan, P.G., Moore, C.J., Eriksen, M., Borerro, J.C., Carson, H.S., ... Thiel, M., 2014. Plastic pollution in the world's oceans: more than 5 trillion plastic pieces weighing over 250,000 tons afloat at sea. PLoS ONE 9 (12), e111913. https://doi.org/10.1371/journal.pone.0111913.

Galgani, François, Hanke, G., Maes, T., 2015. Global distribution, composition and abundance of marine litter. Marine Anthropogenic Litter. Springer International Publishing, Cham, pp. 29–56 https://doi.org/10.1007/978-3-319-16510-3_2.
Galgani, F., Leaute, J.P., Moguedet, P., Souplet, A., Verin, Y., Carpentier, A., ... Nerisson, P., 2000. Litter on the sea floor along European coasts. Mar. Pollut. Bull. https://doi.org/10.1016/S0025-326X(99)00234-9.
Geyer, R., Jambeck, J.R., Law, K.L., 2017. Production, use, and fate of all plastics ever made. Sci. Adv. https://doi.org/10.1126/sciadv.1700782.
Guest, D., Cranmer, K., Whiteson, D., 2018. Deep learning and its application to LHC physics. Annu. Rev. Nucl. Part. Sci. 68 (1), 161–181. https://doi.org/10.1146/annurev-nucl-101917-021019.
Hengstmann, E., Gräwe, D., Tamminga, M., Fischer, E.K., 2017. Marine litter abundance and distribution on beaches on the Isle of Rügen considering the influence of exposition, morphology and recreational activities. Mar. Pollut. Bull. 115 (1–2), 297–306. https://doi.org/10.1016/J.MARPOLBUL.2016.12.026.
Imhof, H.K., Sigl, R., Brauer, E., Feyl, S., Giesemann, P., Klink, S., ... Laforsch, C., 2017. Spatial and temporal variation of macro-, meso- and microplastic abundance on a remote coral island of the Maldives, Indian Ocean. Mar. Pollut. Bull. 116 (1–2), 340–347. https://doi.org/10.1016/j.marpolbul.2017.01.010.
Jambeck, J.R., Geyer, R., Wilcox, C., Siegler, T.R., Perryman, M., Andrady, A., ... Law, K.L., 2015. Marine pollution. Plastic waste inputs from land into the ocean. Science (New York, N.Y.) 347 (6223), 768–771. https://doi.org/10.1126/science.1260352.
Kako, S., Isobe, A., Seino, S., Kojima, A., 2010. Inverse estimation of drifting-object outflows using actual observation data. J. Oceanogr. https://doi.org/10.1007/s10872-010-0025-9.
Kako, S., Isobe, A., Magome, S., 2012. Low altitude remote-sensing method to monitor marine and beach litter of various colors using a balloon equipped with a digital camera. Mar. Pollut. Bull. 64 (6), 1156–1162. https://doi.org/10.1016/j.marpolbul.2012.03.024.
Kako, S., Isobe, A., Kataoka, T., Hinata, H., 2014. A decadal prediction of the quantity of plastic marine debris littered on beaches of the East Asian marginal seas. Mar. Pollut. Bull. https://doi.org/10.1016/j.marpolbul.2014.01.057.
Kataoka, T., Murray, C.C., Isobe, A., 2018. Quantification of marine macro-debris abundance around Vancouver Island, Canada, based on archived aerial photographs processed by projective transformation. Mar. Pollut. Bull. 132 (September 2017), 44–51. https://doi.org/10.1016/j.marpolbul.2017.08.060.
Kiszka, J.J., Mourier, J., Gastrich, K., Heithaus, M.R., 2016. Using unmanned aerial vehicles (UAVs) to investigate shark and ray densities in a shallow coral lagoon. Mar. Ecol. Prog. Ser. 560, 237–242. https://doi.org/10.3354/meps11945.
Laist, D.W., 1987. Overview of the biological effects of lost and discarded plastic debris in the marine environment. Mar. Pollut. Bull. https://doi.org/10.1016/S0025-326X(87)80019-X.
Laist, D.W., 2011. Impacts of Marine Debris: Entanglement of Marine Life in Marine Debris Including a Comprehensive List of Species With Entanglement and Ingestion Records. https://doi.org/10.1007/978-1-4613-8486-1_10.
Lavers, J.L., Bond, A.L., 2017. Exceptional and rapid accumulation of anthropogenic debris on one of the world's most remote and pristine islands. Proc. Natl. Acad. Sci. 114 (23), 6052–6055. https://doi.org/10.1073/pnas.1619818114.
Lavers, J.L., Oppel, S., Bond, A.L., 2016. Factors influencing the detection of beach plastic debris. Mar. Environ. Res. https://doi.org/10.1016/j.marenvres.2016.06.009.
Law, K.L., Morét-Ferguson, S., Maximenko, N.A., Proskurowski, G., Peacock, E.E., Hafner, J., Reddy, C.M., 2010. Plastic accumulation in the North Atlantic subtropical gyre. Science https://doi.org/10.1126/science.1192321.
Law, K.L., Morét-Ferguson, S.E., Goodwin, D.S., Zettler, E.R., Deforce, E., Kukulka, T., Proskurowski, G., 2014. Distribution of surface plastic debris in the eastern pacific ocean from an 11-year data set. Environ. Sci. Technol. https://doi.org/10.1021/es4053076.
Lebreton, L.C.M., Van Der Zwet, J., Damsteeg, J.W., Slat, B., Andrady, A., Reisser, J., 2017. River plastic emissions to the world's oceans. Nat. Commun. 8, 1–10. https://doi.org/10.1038/ncomms15611.
Lebreton, L., Slat, B., Ferrari, F., Sainte-Rose, B., Aitken, J., Marthouse, R., ... Reisser, J., 2018. Evidence that the Great Pacific Garbage Patch is rapidly accumulating plastic. Sci. Rep. 8 (1), 1–15. https://doi.org/10.1038/s41598-018-22939-w.
LeCun, Y., Bengio, Y., Hinton, G., 2015. Deep learning. Nature 521 (7553), 436–444. https://doi.org/10.1038/nature14539.
Levy, J., Hunter, C., Lukacazyk, T., Franklin, E.C., 2018. Assessing the spatial distribution of coral bleaching using small unmanned aerial systems. Coral Reefs, 1–15 https://doi.org/10.1007/s00338-018-1662-5.
Martin, C., Parkes, S., Zhang, Q., Zhang, X., McCabe, M.F., Duarte, C.M., 2018. Use of unmanned aerial vehicles for efficient beach litter monitoring. Mar. Pollut. Bull. 131, 662–673. https://doi.org/10.1016/j.marpolbul.2018.04.045.
Mheen, M., Pattiaratchi, C., Sebille, E., 2019. Role of Indian Ocean dynamics on accumulation of buoyant debris. J. Geophys. Res. Oceans, 2018JC014806 https://doi.org/10.1029/2018JC014806.
Mlambo, R., Woodhouse, I.H., Gerard, F., Anderson, K., 2017. Structure from motion (SfM) photogrammetry with drone data: a low cost method for monitoring greenhouse gas emissions from forests in developing countries. Forests 8 (3), 68. https://doi.org/10.3390/f8030068.
Thompson, Richard C., Olsen, Ylva, Mitchell, Richard P., Davis, Anthony, Rowland, Steven J., John, Anthony W.G., Mcgonigle, Daniel, Russell, A.E., Thompson, R.C., Olsen, Y., Mitchell, R.P., Davis, A., Rowland, S.J., ... Russell, A.E., 2004. Lost at sea: where is all the plastic? Science https://doi.org/10.1126/science.1094559.
Penca, J., 2018. European Plastics Strategy: what promise for global marine litter? Mar. Policy 97, 197–201. https://doi.org/10.1016/J.MARPOL.2018.06.004.
Pierdomenico, M., Casalbore, D., Chiocci, F.L., 2019. Massive benthic litter funnelled to deep sea by flash-flood generated hyperpycnal flows. Sci. Rep. 9 (1), 5330. https://doi.org/10.1038/s41598-019-41816-8.
Programme, U. N. E, 2005. Marine Litter an Analytical Overview www.unep.org. Retrieved from. http://wedocs.unep.org/handle/20.500.11822/8348.
Ramirez-Llodra, E., De Mol, B., Company, J.B., Coll, M., Sardà, F., 2013. Effects of natural and anthropogenic processes in the distribution of marine litter in the deep Mediterranean Sea. Prog. Oceanogr. https://doi.org/10.1016/j.pocean.2013.07.027.
Rochman, C.M., Browne, M.A., Halpern, B.S., Hentschel, B.T., Hoh, E., Karapanagioti, H.K., ... Thompson, R.C., 2013. Policy: classify plastic waste as hazardous. Nature https://doi.org/10.1038/494169a.
Ryan, P.G., 2015. A brief history of marine litter research. Marine Anthropogenic Litter https://doi.org/10.1007/978-3-319-16510-3_1.
Ryan, P.G., Moore, C.J., Van Franeker, J.A., Moloney, C.L., 2009. Monitoring the abundance of plastic debris in the marine environment. Philos. Trans. R. Soc. B 364 (1526), 1999–2012. https://doi.org/10.1098/rstb.2008.0207.
Saliu, F., Montano, S., Garavaglia, M.G., Lasagni, M., Seveso, D., Galli, P., 2018. Microplastic and charred microplastic in the Faafu Atoll, Maldives. Mar. Pollut. Bull. 136, 464–471. https://doi.org/10.1016/j.marpolbul.2018.09.023.
Saliu, F., Montano, S., Leoni, B., Lasagni, M., Galli, P., 2019. Microplastics as a threat to coral reef environments: detection of phthalate esters in neuston and scleractinian corals from the Faafu Atoll, Maldives. Mar. Pollut. Bull. 142, 234–241. https://doi.org/10.1016/j.marpolbul.2019.03.043.
Savini, A., Vertino, A., Marchese, F., Beuck, L., Freiwald, A., 2014. Mapping cold-water coral habitats at different scales within the Northern Ionian Sea (Central Mediterranean): an assessment of coral coverage and associated vulnerability. PLoS One 9 (1), e87108. https://doi.org/10.1371/journal.pone.0087108.
Sha, J., Shifaw, E., Bao, Z., Li, X., Hanchiso, T., 2018. Monitoring of beach litter by automatic interpretation of unmanned aerial vehicle images using the segmentation threshold method. Mar. Pollut. Bull. 137, 388–398. https://doi.org/10.1016/j.marpolbul.2018.08.009.
Shimizu, T., Nakai, J., Nakajima, K., Kozai, N., Takahashi, G., Matsumoto, M., Kikui, J., 2008. Seasonal variations in coastal debris on Awaji Island, Japan. Mar. Pollut. Bull. https://doi.org/10.1016/j.marpolbul.2007.10.005.
Thiel, M., Hinojosa, I.A., Miranda, L., Pantoja, J.F., Rivadeneira, M.M., Vásquez, N., 2013. Anthropogenic marine debris in the coastal environment: a multi-year comparison between coastal waters and local shores. Mar. Pollut. Bull. 71 (1–2), 307–316. https://doi.org/10.1016/J.MARPOLBUL.2013.01.005.
Thompson, R.C., Moore, C.J., Saal, F.S.V., Swan, S.H., 2009. Plastics, the environment and human health: current consensus and future trends. Philos. Trans. R. Soc. B https://doi.org/10.1098/rstb.2009.0053.
UNEP, 1999. Western Indian Ocean Environment Outlook-1999. UNEP, Nairobi.
Van Cauwenberghe, L., Vanreusel, A., Mees, J., Janssen, C.R., 2013. Microplastic pollution in deep-sea sediments. Environ. Pollut. https://doi.org/10.1016/j.envpol.2013.08.013.
Ventura, D., Bruno, M., Jona Lasinio, G., Belluscio, A., Ardizzone, G., 2016. A low-cost drone based application for identifying and mapping of coastal fish nursery grounds. Estuar. Coast. Shelf Sci. 171, 85–98. https://doi.org/10.1016/j.ecss.2016.01.030.
Ventura, D., Bonifazi, A., Gravina, M.F., Belluscio, A., Ardizzone, G., 2018. Mapping and classification of ecologically sensitive marine habitats using unmanned aerial vehicle (UAV) imagery and Object-Based Image Analysis (OBIA). Remote Sens. 10 (9), 1331. https://doi.org/10.3390/rs10091331.
Verhoeven, G., 2011. Taking computer vision aloft - archaeological three-dimensional reconstructions from aerial photographs with photoscan. Archaeol. Prospect. 18 (1), 67–73. https://doi.org/10.1002/arp.399.
Vlachogianni, T., Fortibuoni, T., Ronchi, F., Zeri, C., Mazziotti, C., Tutman, P., ... Scoullos, M., 2018. Marine litter on the beaches of the Adriatic and Ionian Seas: an assessment of their abundance, composition and sources. Mar. Pollut. Bull. 131, 745–756. https://doi.org/10.1016/J.MARPOLBUL.2018.05.006.
Watts, A.J.R., Porter, A., Hembrow, N., Sharpe, J., Galloway, T.S., Lewis, C., 2017. Through the sands of time: beach litter trends from nine cleaned north cornish beaches. Environ. Pollut. https://doi.org/10.1016/j.envpol.2017.05.016.